

DIRECT NUMERICAL SIMULATION ON LAMINARIZATION OF TURBULENT FORCED GAS FLOWS IN CIRCULAR TUBES WITH STRONG HEATING

Shin-ichi Satake

Dept. of Mechanical System Engineering, Toyama University
Toyama, Toyama, 930-0887, Japan

Tomoaki Kunugi

Dept. of Nuclear Engineering, Kyoto University
Yoshida, Sakyo, Kyoto, 606-8501, Japan

A. Mohsen Shehata

Xerox Corporation, 800 Phillips Road, 311-20N, Webster, N.Y. 14580, U.S.A.

Donald M. McEligot

Idaho National Engineering and Environmental Laboratory, Idaho Falls, Idaho 83415-3885, USA
and University of Arizona, Tucson, Arizona 85721 USA

ABSTRACT

A direct numerical simulation (DNS) with turbulent transport of a variable property fluid has been carried out to grasp and understand the laminarization phenomena caused by strong heating. In this study, the inlet Reynolds number based on a bulk velocity and a pipe diameter was set to be constant at $Re=4300$. The temperature distribution taken from the experiments by Shehata and McEligot (1998) was applied to the wall as a thermal boundary condition. The number of computational nodes used in this study was $768 \times 64 \times 128$ in the z -, r - and ϕ - directions, respectively. The turbulent quantities such as the mean flow, temperature fluctuations, turbulent stresses and the turbulent statistics were obtained via DNS. The turbulent drag decreases along the streamwise direction. The cause of this reduction can be considered that the fluid behavior changes drastically in the near wall region due to strong heating.

INTRODUCTION

General effects of strong heating of a gas are variation of the transport properties, reduction of density causing acceleration of the flow in the central core, and - in some cases - significant buoyancy forces. Growth of the internal thermal boundary layer leads to readjustment of any previously fully-developed turbulent momentum profile. No truly fully-established conditions are reached because the

temperature rises -- leading, in turn, to continuous axial and radial variation of properties such as the gas viscosity. In an application such as the High Temperature Test Reactor (HTTR) in Japan (or reduction of flow scenarios in other plants) another complication arises. To obtain high outlet temperatures, design gas flow rates are kept relatively low. For example, at the exit of the HTTR (Takase et al., 1990) cooling channels, the Reynolds number is about 3500. In this range the heat transfer parameters may appear to correspond to turbulent flow or to laminar flow or to an intermediate behavior, depending on the heating rate (Bankston, 1970), with consequent differences in their magnitudes. The situation where laminar values are measured at Reynolds numbers typifying turbulent flow is called "laminarization" by some authors. For further general background on laminarization in internal convective heat transfer to gases, a survey by McEligot (1986) may be useful.

For dominant forced convection with significant gas property variation, in low Mach number flow of common gases through a circular tube, until recently apparently the only published profile data available to guide (or test) the development of predictive turbulence models have been Perkin's measurements (1975) of mean temperature distributions. Shehata and McEligot (1998) obtained the first mean velocity distributions for this situation. The few "advanced" turbulence models applied for high heating rates (Kawamura, 1979; Fujii et al., 1991; Torii et al., 1993; Torii and Yang, 1997) were developed *without* the benefit of

velocity and temperature distributions in strongly-heated, dominant forced flow for guidance or testing. None of these investigators appear to have compared their predictions to internal data for strongly-heated gas flows. To the authors' knowledge, the only numerical studies of 'advanced' turbulence models for turbulent and laminarizing flows at high heating rates that utilized internal data have been those of Mikieliewicz (1994), Ezato et al. (1997) and Nishimura et al. (1997) which employed measurements from Shehata and McEligot (1998).

In the present study, the DNS for the turbulent pipe flow with strong heating has been carried out by means of the finite volume method developed by Satake and Kunugi (1998a, 1998b). The turbulent statistics for the mean velocity, velocity fluctuations and heat transfer coefficients are predicted and compared with careful measurements (Shehata and McEligot, 1998) for the same conditions. Furthermore, the budget of turbulent kinetic energy and turbulent structures are presented.

SOLUTION PROCEDURE

The DNS code with cylindrical coordinates can numerically solve the continuity and momentum equations using the radial momentum flux formulation. A second-order finite volume discretization scheme is applied to the spatial derivatives on a staggered mesh system in order to avoid a singularity at the center axis of the pipe (Verzicco and Orlandi, 1996). The incompressible Navier-Stokes and continuity equations described in cylindrical coordinates are integrated in time by using the fractional-step method (Dukowicz and Dvinsky, 1992). A second-order Crank-Nicholson scheme is applied to the radial direction terms and a modified third-order Runge-Kutta scheme (Spalart et al., 1991) is used for other terms. In our previous study regarding constant-property, turbulent pipe flow (Satake and Kunugi, 1998a, 1998b), this DNS code has shown good agreement with the existing DNS results.

COMPUTATIONAL CONDITIONS

The computational domain consists of two parts, i.e., an inflow generator which provides the inlet DNS flow and a main part which corresponds to the experimental set-up.

The pipe length of the main part is the same as in the experiment (Shehata and McEligot, 1998) shown in Figure 1. The experimental data are provided as bases for comparison with the computational results. The inlet Reynolds number based on the bulk velocity and viscosity at the exit of the inflow generator and the pipe diameter (D) is assumed to be 4300. This condition corresponds to the RUN 445 of the experiments. Air is the working fluid. Thermal properties are evaluated as power-law functions of the pointwise temperature and pressure with density estimated via the perfect gas approximation as by Perkins (1975). Uniform

mesh spacing is applied to the circumferential (ϕ) and the streamwise (z) directions. As for the radial direction (r), non-uniform mesh spacing specified by a hyperbolic tangent function is employed. The number of grid points is $768 \times 64 \times 128$ in the z -, r - and ϕ -directions, respectively. The inlet boundary condition is provided by the inflow generator; that is, a fully-turbulent pipe flow with constant fluid properties is considered at the entry. The number of computational nodes for the inflow generator is $128 \times 64 \times 128$ points in the z -, r - and ϕ -directions, respectively. A convective boundary condition (Lowery et al., 1987) is imposed at the exit of the main computational domain. One should note that the mass balance between inflow and outflow must be maintained at every time step. As for the thermal boundary condition, the temperature distribution along the pipe wall was specified, based on the data. Although a constant heat flux was applied as the thermal boundary condition in the experiment, it is difficult to treat a constant heat flux condition for spatial developing flow problems with the present DNS techniques (Satake and Kunugi, 1998c). Therefore, this DNS is focused on the investigation of the turbulent heat and momentum transfer mechanisms in a pipe with a known wall temperature distribution.

RESULTS AND DISCUSSION

Figure 2 shows the relationship between the local integral Stanton number and the bulk Reynolds number. The Reynolds number is 4300 at the inlet region and decreases to about 3000 at the outlet. The present DNS results show fairly good agreement with the data (Shehata and McEligot, 1998).

The non-dimensional static pressure drop is shown in Fig. 3. Agreement of the present result with the experiment is good. In Fig. 4, the bulk temperature rise shows excellent agreement with experiment. Figures 5(a)–(c) present the comparisons of mean axial velocity profiles normalized by bulk velocity. The comparisons are made at three representative locations, $z/D=3.2$, $z/D=14.2$ and $z/D=24.5$, and show mostly excellent agreement.

Figure 6 shows the predicted distributions of Reynolds shear stress. The solid line shows the DNS without heating and the solid and open symbols represent the results of a $k-\epsilon$ model (Ezato et al., 1997) and a RSM model (Nishimura et al., 1997), respectively. The DNS results are fairly in good agreement with the $k-\epsilon$ model. However, the RSM results are relatively smaller than the DNS and the $k-\epsilon$ model. This difference might be caused by the low Reynolds approximations in the RSM and $k-\epsilon$ model. Figure 7 shows the distributions of streamwise velocity fluctuations. It is interesting that the streamwise component obtained by the DNS with heating shows the same trends as the RSM. Figure 8 shows the distributions of radial velocity fluctuations. The values are small in all regions because the effect of property change on the radial component is very strong. Figure 9 shows the distributions of circumferential

velocity fluctuations and they indicate the same trend as the radial component. Thus, the turbulence behavior in the DNS with heating tends to be more isotropic than that without heating, and the magnitudes of the radial and circumferential velocity fluctuating components are roughly the same. The predicted budgets of turbulent kinetic energy are shown in Figs. 10(a)-(c) for $z/D=3.2$, 14.2 and 24.5, respectively. Near the entry ($z/D \approx 3$) convection and buoyant terms obtained by the DNS are observed and are very pronounced in the location of peak value of the production term. Although convection and buoyant terms exist in the budget, the overall profiles of all terms are not very different from the DNS without heating (Satake and Kunugi, 1998a). Negative gradients in viscous and dissipation terms at the wall are also observed in Figs. 10 (a)-(b). A similar tendency due to laminarization can be observed in the DNS results for a very low Reynolds number channel by Iida et al.(1997). All terms decay in the downstream direction. At $z/D=24.5$, all terms nearly disappear.

The predicted spatial evolution of the flow field with strong heating is visualized sequentially in Figs. 11 (a) for $z/D=0-5$, (b) 5-10, (c) 10-15, (d) 15-20 and (e) 20-25. The gray and black contour surfaces in the half-cut view of the pipe represent the low-pressure and low-speed regions corresponding to the vortical structure and wall-layer streaks, respectively. Within the first section ($z/D=0-5$), these structures are quite different from those of pipe flow without heating (Satake and Kunugi, 1998a). However, the low-pressure regions representing the vortical structures decay rapidly at $z/D > 5$. The vortical structures disappear in this region and the low-speed streaks and their meandering become weak. One may recall that the meandering of streaks is a dominant phase in the ordinary turbulence regeneration processes (Hamilton et al., 1995). Thus, in the initial heated region ($z/D=0-5$), the turbulence is suppressed as a consequence of the property change and it is not regenerated in the downstream region.

CONCLUDING REMARKS

Direct numerical simulations for turbulent pipe flow with strong heating were carried out. It is shown that the resulting large thermal property change of working fluid leads to a remarkable drag reduction of the initially turbulent pipe flow. The turbulent fluctuations decrease mostly after five to ten diameters in the downstream direction. Furthermore, visualized vortical and streaky structures decay in the downstream region.

REFERENCES

Bankston, C. A., 1970, The transition from turbulent to laminar gas flow in a heated pipe, *J.Heat Transfer*, **92**, pp.569-579.
 Dukowicz, J. K. and Dvinsky, A. S., 1992, Approximate factorization as a high order splitting for the implicit

incompressible flow equations, *J. Comp. Phys.*, **102**, No.2, pp. 336-347.
 Ezato, K., Shehata, A. M., Kunugi, T. and McEligot, D. M., 1997, Numerical predictions of transitional features of turbulent gas flows in circular tubes with strong heating, Paper FEDSM97-3304, ASME Fluids Eng. Conf., Vancouver, B. C.
 Fujii, S., Akino, N., Hishida, M., Kawamura, H. and Sanokawa, K., 1991, Experimental and theoretical investigations on heat transfer of strongly heated turbulent gas flow in an annular duct, *JSME International J., Ser II*, **34**, No. 3, pp. 348-354.
 Hamilton, J., Kim, J. and Waleffe, F., 1995, Regeneration mechanisms of near-wall turbulence structures, *J Fluid Mech.*, **287**, pp.317-348.
 Iida, O., Ohtsuka, A. and Nagano, Y., 1997, The drag reduction mechanisms in the retransition of turbulent channel flow, Proc., 2th Int. Symp. on Turbulence, Heat and Mass Transfer, pp. 209-218.
 Kawamura, H., 1979, Analysis of laminarization of heated turbulent gas using a two-equation model of turbulence, Proc., 2nd Intl. Symp. Turb. Shear Flow, London, pp.18,16-18,21.
 Lowery, P.S., Reynolds, W.C. and Mansour, N.N., 1987, Passive scalar entrainment and mixing in a forced spatially-developing mixing layer, AIAA paper, 87-0142.
 McEligot, D. M., 1986, Convective heat transfer in internal gas flows with temperature-dependent properties, *Adv. Transport Processes*, **4**, pp 113-200.
 Mikielewicz, D. P., 1994, Comparative studies of turbulence models under conditions of mixed convection with variable properties in heated vertical tubes, Ph.D. thesis, Univ. Manchester.
 Nishimura, M., Fujii, S., Shehata, A.M., Kunugi, T. and McEligot, D.M., 1997, Prediction of forced gas flows in circular tubes at high heat fluxes, Proc., 8th international topical meeting on nuclear reactor thermal-hydraulics, Kyoto, pp. 294-304.
 Perkins, K. R., 1975, Turbulence structure in gas flows laminarizing by heating, Ph.D. thesis, Univ. Arizona.
 Satake, S. and Kunugi, T., 1998a, Direct numerical simulation of turbulent pipe flow, *Bulletin, JSME*, **64**, pp. 65-70 (in Japanese).
 Satake, S. and Kunugi, T., 1998b, Direct numerical simulation of an impinging jet into parallel disks. *Int. J. Num. Method sHeat Fluid Flow*, **8**, pp.768-780.
 Satake, S. and Kunugi, T., 1998c, Direct numerical simulation of turbulent pipe flow with nonuniform surface heat flux, *Thermal Sci. Eng.*, **6**, No. 2, pp. 1-7 (in Japanese).
 Shehata, A. M., and McEligot, D.M., 1998, Mean turbulence structure in the viscous layer of strongly-heated internal gas flows. Measurements, *Int. J. Heat Mass Transfer*, **41**, pp. 4297-4313.
 Spalart, P.R., Moser, R. D. and Rogers, M. M , 1991, Spectral methods for the Navier-Stokes equations with one infinite and two periodic directions, *J. Comp. Phys.*, **96**, pp. 297-324.
 Takase, K., Hino, R. and Miyamoto, Y., 1990, Thermal and hydraulic tests of standard fuel rod of HTTR with HENDEL. *J. Atomic Energy Soc. Japan*, **32-11**, pp.1107-1110 (in Japanese).

Torii, S., Shimizu, A., Hasegawa, S. and Higasa, M., 1993, Numerical analysis of laminarizing circular tube flows by means of a Reynolds stress turbulence model, *Heat Transfer - Japanese Research*, **22**, pp. 154-170.

Torii, S., and Yang, W.-J., 1997, Laminarization of turbulent gas flow inside a strongly heated tube. *Int. J. Heat Mass Transfer*, **40**, pp. 3105-3117.

Verzicco, R. and Orlandi, P., 1996, A finite-difference scheme for three-dimensional incompressible flows in cylindrical coordinate, *J. Comp. Phys.*, **123**, pp. 402-414.

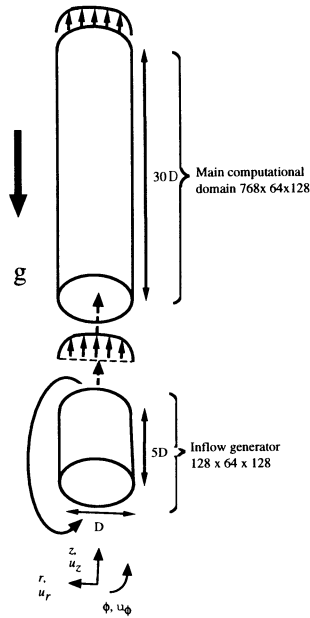


Figure 1. Coordinate System and Boundary Conditions

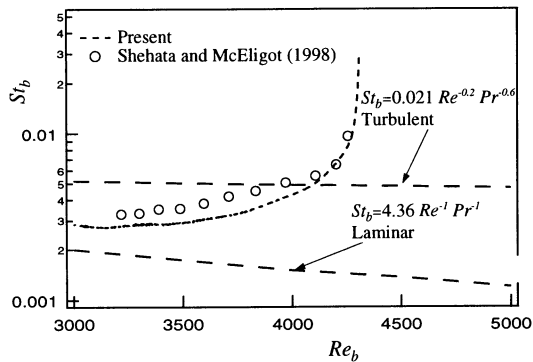


Figure 2. The relationship between the local integral Stanton number and the bulk Reynolds number.

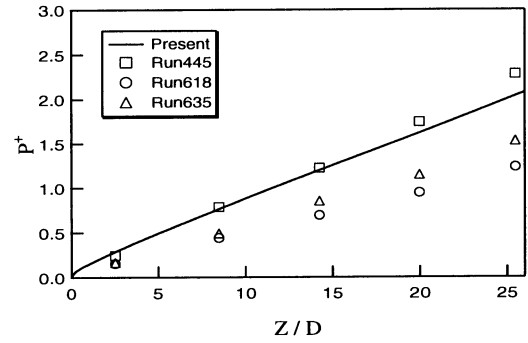


Figure 3. Comparison of static pressure

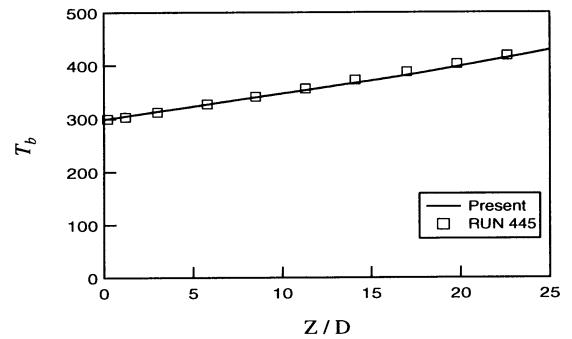


Figure 4. The bulk temperature

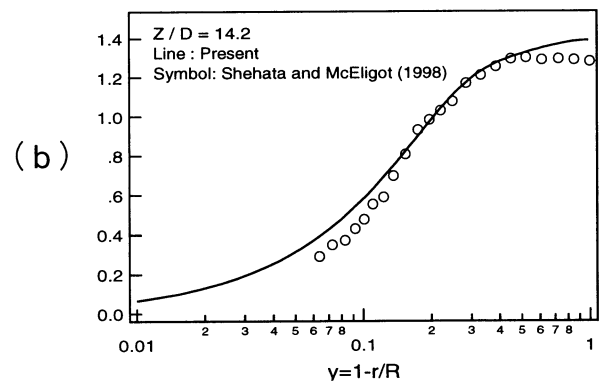
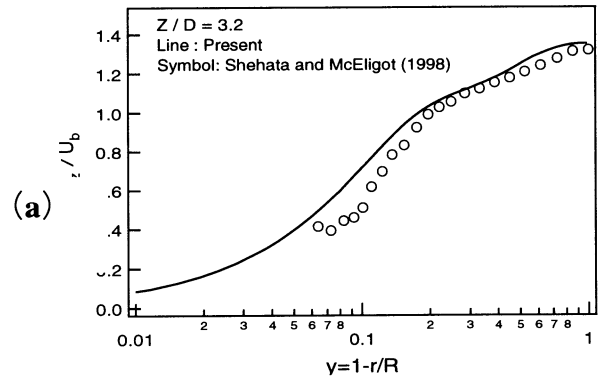


Figure 5. Mean velocity profiles

(c)

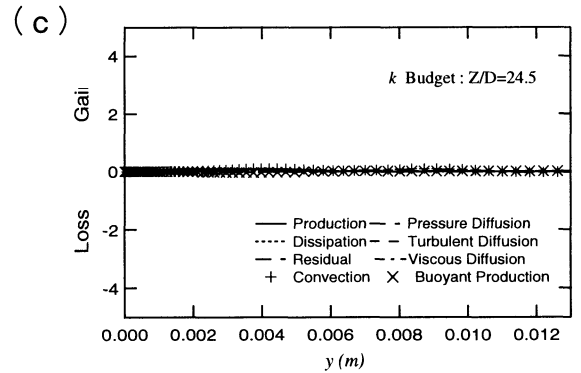
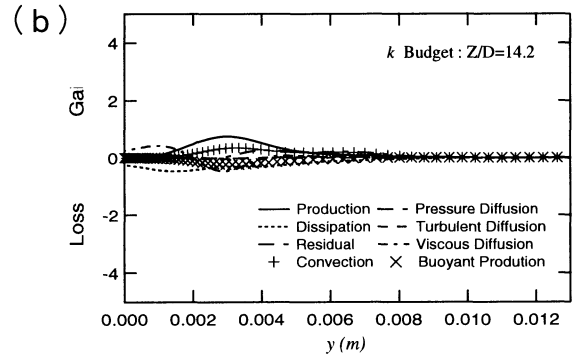
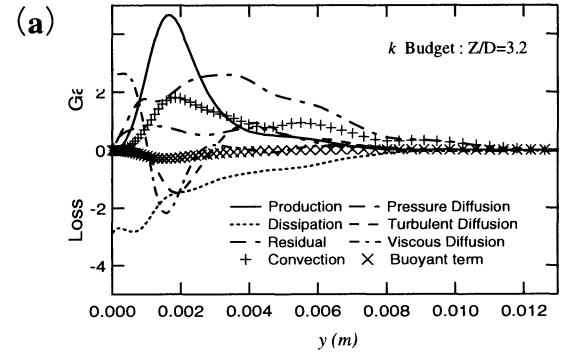
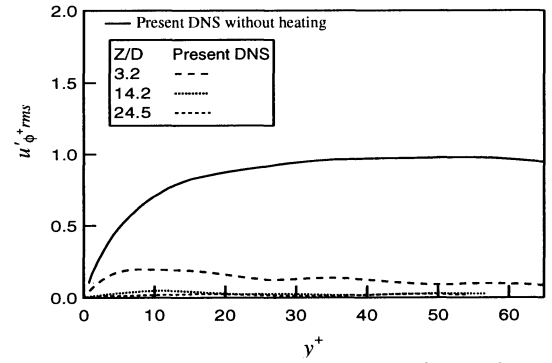
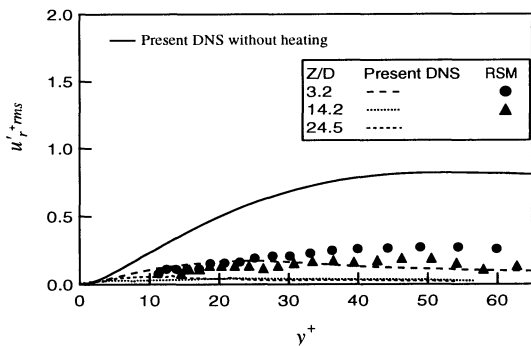
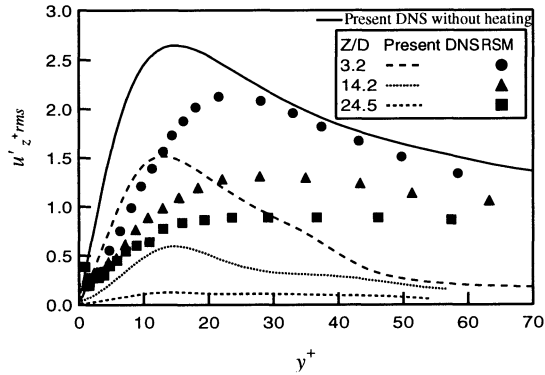
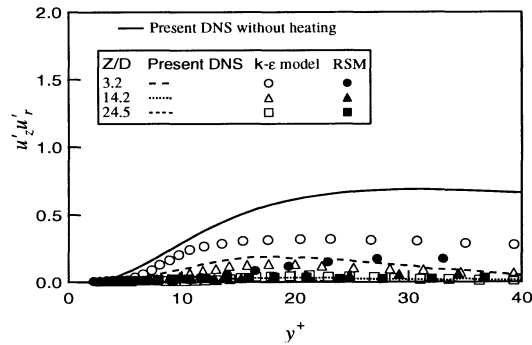
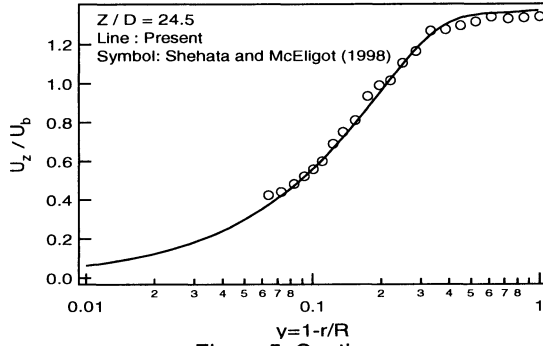


Figure 10. Turbulent kinetic energy budget

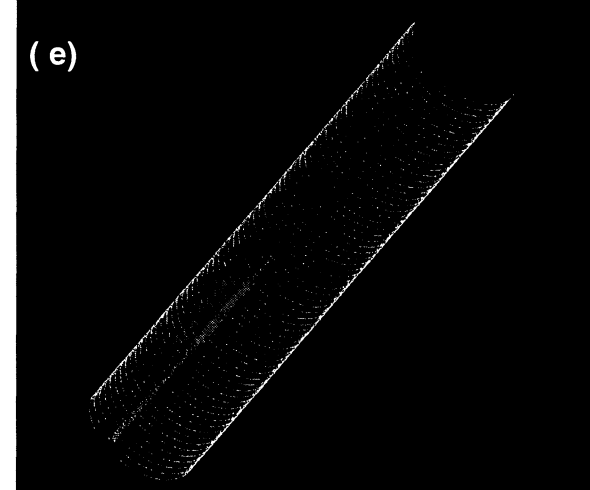
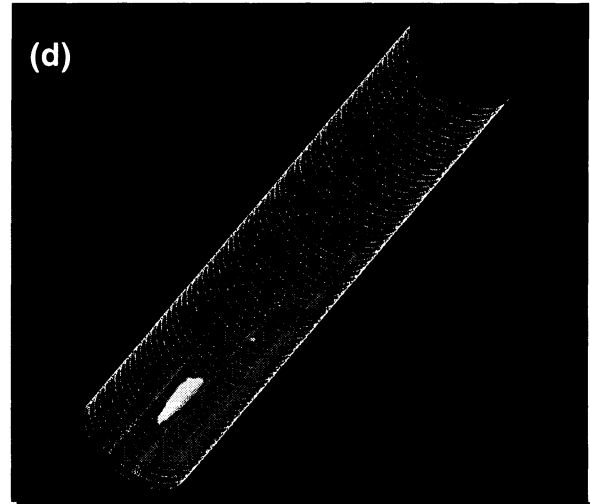
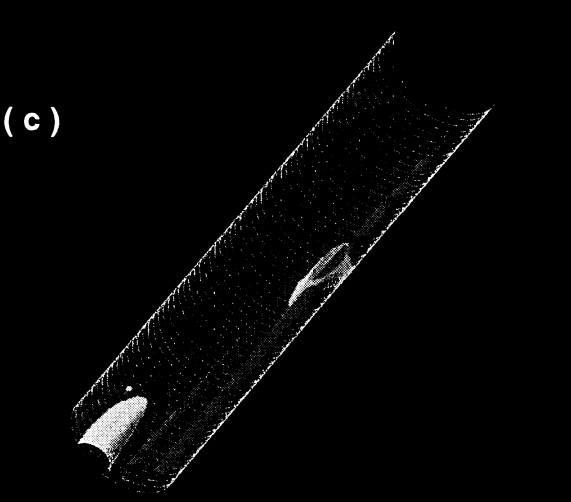
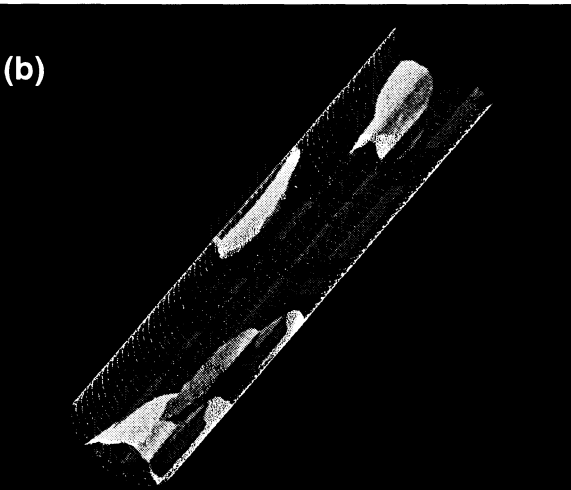
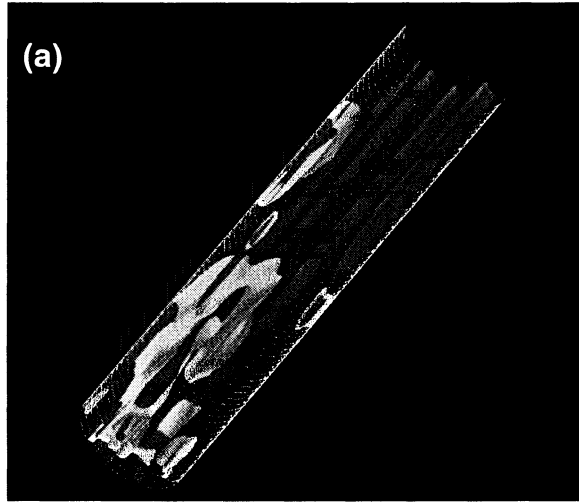


Figure 11. Contour surface of low-pressure and low-speed regions with high heating: (a) gray, $p' < -0.1$ [Pa] ; gray, $u_z' < -0.35$ [m/s] (at $Z/D=0$ to 5); (b) gray, $p' < -0.01$ [Pa] ; gray, $u_z' < -0.35$ [m/s] (at $Z/D=5$ to 10); (c) gray, $p' < -0.01$ [Pa] ; gray, $u_z' < -0.35$ [m/s] (at $Z/D=10$ to 15); (d) gray, $p' < -0.01$ [Pa] ; gray, $u_z' < -0.2$ [m/s] (at $Z/D=15$ to 20); (e) gray, $p' < -0.01$ [Pa] ; gray, $u_z' < -0.15$ [m/s] (at $Z/D=15$ to 20).